Experimental and numerical study on the R744 ejector with a suction nozzle bypass

Jakub Bodys[a,*], Jacek Smolka[a], Michal Palacz[a],
Michal Haida[a], Krzysztof Banasiak[b], Andrzej J. Nowak[a]

[a] *Silesian University of Technology, Gliwice, 44-100, Poland*
[b] *Norwegian University of Science and Technology, Trondheim, 7465, Norway*

Abstract

State-of-the-art R744 cooling cycles include highly efficient ejectors as a crucial element for competitive energy consumption in warm climates. However, an improvement is still possible, as shown in this study. This study is the first to experimentally investigate a construction of the R744 ejector with a modulated opening of the suction nozzle bypass duct. Four bypass positions along the ejector axis were tested using three sets of motive nozzle conditions characteristic of a refrigeration unit operating in a warm climate. Two levels of evaporation temperature, as well as the superheat influence, were investigated to evaluate the application potential. The efficiency of the prototype was equal to or greater than that of the standard construction because the closed bypass duct did not result in deteriorated ejector performance. The best bypass positioning resulted in improved efficiency for the pressure lift up to 7 bar. The maximum efficiency improvement was 37% with application potential for systems with low-pressure lift modes. The simulation of the full 3-D bypass ejector allowed for insight into the efficiency improvement. Finally, guidelines were given for further improvement considering the connection between the standard suction chamber and the bypass chamber.

Keywords: R744 ejector, experimental tests, performance improvement, bypass, numerical analysis

Nomenclature

Abbreviations

$\dot{W}$	Expansion work rate	W
D	Diameter	m
d	Width	m
h	Specific enthalpy	$J{\cdot}kg^{-1}$
L	Length	m

* Corresponding author
Email address: jakub.bodys@polsl.pl {+48322372341} (Jakub Bodys)

m	Mass flow rate	kg·s^{-1}
p	Absolute pressure	Pa
s	Specific entropy	J·kg^{-1}· K^{-1}
Subscripts		
β, γ	Angle	°
χ	Mass entrainment ratio	-
δ_m	Relative error of the mass flow rate	%
η	Efficiency	-
Ψ	Dimensionless position of the bypass duct along the ejector axis	-
Superscripts		
bps	Bypass	-
CFD	Computational Fluid Dynamics	-
DIFF	Diffuser	-
ej	Ejector	-
EXP	Experimental	-
g	Saturated gas	-
l	Saturated liquid	-
max	Maximum	-
mix	Mixer	-
MN	Motive nozzle	-
OUT	Outlet	-
rec	Recovered expansion work	-
sat	Saturation state	-
SIM	Simulation	-
SN	Suction nozzle	-
Roman Symbols		
CO_2, R744	Carbon dioxide	-
HEM	Homogeneous equilibrium model	-
HPV	Expansion valve	-
HVAC&R	Heating, ventilation, air conditioning refrigeration	-
IHX	Internal heat exchanger	-

1. Introduction

1.1. State-of-the-art R744 HVAC&R systems

Intensive research on carbon dioxide (R744) cooling technology as a standard solution in mobile applications with wide potential for large-scale heating, ventilation, air conditioning and refrigeration (HVAC&R) was proposed over two decades ago [1]. Carbon dioxide installations present substantial benefits in the form of unit compactness, easily accessible cooling-heating integration and inexpensive and unlimited availability concerning current and future legal requirements [2, 3, 4, 5]. Innovative HVAC&R systems based on R744 became a standard solution for supermarkets [6], as well as a domestic solution for heat pumps [7]. The R744 development provided integrated solutions for hotels [8], office buildings [9] and even entire islands, such as Mauritius [10].

A crucial and common feature in state-of-the-art R744 cooling and heating technology is the implementation of ejectors to the system layout [11], which brings substantial differences between particular CO2-based systems [12]. The study presented by Gullo et al. [13] underlined the substantial influence of the R744 transcritical ejector cycles in overcoming challenging applications in warm climates. Furthermore, according to Gullo et al. [14], the next generations of large-scale R744 systems with the integration of heating and cooling purposes should be based on cutting-edge ejector solutions. Moreover, the potential for R744 cycles in various operating conditions is continuously explored in areas outside standard HVACR applications. For example, cryogenic cooling cycles involving ejectors were investigated in [15], while advanced systems of energy storage with condensing ejectors were presented in [16].

1.2. Regulation and control strategies of the ejector performance

Considering the importance of ejector utilisation in R744 systems, several research areas could be indicated. Namely, the design process, control strategies and continuously growing number of cycle configurations, including those in commercial applications, were underlined in the comprehensive review presented by Elbel and Lawrence [17]. This paper presented a rapid development of the ejector research field that could be captured in significant improvement of the design tools starting from the first 1-D models to advanced approaches based on computational fluid dynamics (CFD) methods. Furthermore, strategies and mechanisms of ejector control were underlined as a key aspect for further development because of numerous applications in which off-design conditions are inevitable. As a consequence of this operation, the ejector performance deteriorates because of degraded mass entrainment.

The first experimental analysis [18] of the control mechanism based on needle implementation into the R744 ejector motive nozzle to regulate ejector performance was characterised as an effective solution. On the other hand, the reduction of the motive nozzle throat in the controllable ejector should be carefully adjusted because of the possibility of choking phenomena along with increased friction related to the increased surface area introduced to the high-speed motive flow area [19].

The multi-ejector concept was presented by Hafner et al. [20] and experimentally investigated by Banasiak et al. [21], while this technology is now available on the commercial market. This solution could be located opposite the fluent needle positioning in the motive nozzle throat and could result in continuous regulation. The multi-ejector approach is based on multiple ejectors operating in parallel and depends on the requested or delivered motive stream. Hence, the regulation of the motive ports is managed in a binary manner by turning on or off the proper ejector regarding its size and operation range. Compared to the controllable ejector, the multi-ejector solution brings the benefits of reduced friction in the motive nozzle and stable performance of the ejectors. However, manufacturing multiple ejectors and control valves involves higher investment costs.

Lawrence and Elbel [22] presented an experimental analysis of control strategies based on the controllable ejector and expansion valves in serial and parallel to the motive port. The comparison revealed the advantage of the adjustable ejector in terms of the ejector efficiency regarding the off-design conditions of ejector operation. On the other hand, the level of this advantage could be lowered regarding the simplicity and low cost of the expansion valves. A novel solution based on vortex introduction to the motive stream through the tangentially introduced duct was proposed and experimentally investigated by Zhu and Elbel [23]. Based on the R134a flow, the authors delivered an analysis of the effective stream control and visualised the resulting expansion jet [23]. Furthermore, the developed mechanism was implemented on the R744 ejector with positive results concerning the ejector performance and the aforementioned effective regulation [24]. The aforementioned studies improved the state-of-the-art knowledge and application potential based on effective motive nozzle regulation in the R744 ejector. On the other hand, each analysed solution of motive stream regulation involves a noticeable pressure loss and lower performance factors compared to those of the on-design conditions.

1.3. Application of the suction nozzle bypass

An unfavourable pressure distribution in the ejector mixing chamber could be present even despite the motive flow regulation in the off-design conditions. The relationship between the motive nozzle, premixing chamber and mixer was investigated in the study presented by Palacz et al. [25], in which comprehensive optimisation of the R744 ejector geometry was provided. The inappropriate dimensions of the mixing section for the given motive nozzle states resulted in high entropy generation in the shock-wave pattern, correlated choking phenomena and finally constrained entrainment. A similar design criterion was confirmed for other working fluids as well [26, 27].

In the off-design conditions, avoidance of the flow with high entropy generation can be realised based on the additional bypass duct where suction flow is introduced at the end or after the mixing section of the ejector. On this basis, the second inlet of the suction nozzle is implemented in the ejector, which is then called a two-stage ejector. However, in this study, the nomenclature of the bypass ejector will be used. In the study presented by Chen et al. [28], the air ejector with bypass was proposed and numerically analysed. Further CFD-based investigations focused on the geometrical and operational factors that influence the performance of the bypass ejector [29]. Depending on the pressure conditions at the ejector ports, the mass entrainment ratio was intensified by up to 32.8%. Moreover, the crucial effect of the geometry and positioning of the bypass duct was emphasized.

The bypass implementation to the ejector with an adjustable motive nozzle throat (spindle insertion) was numerically analysed with methane as a working fluid [30]. The simulation results of a baseline ejector were validated against the data obtained from an industrial natural gas field located in northwestern China. The numerical analysis of the combined ejector with the spindle and the bypass revealed a large potential for improvement of 75.0% compared to the baseline ejector. The same methane ejector was analysed in the study by Chen et al. [31], where the implementation of two separated bypass inlets was considered. The authors analysed various geometrical configurations of the bypass inlets. Moreover, the suction pressure of each bypass inlet was analysed to evaluate the maximum potential in a proper configuration of the serviced natural gas wells. A computed improvement of 48.93% over the aforementioned baseline ejector was obtained.

Tang et al. [32] proposed a steam ejector with the suction nozzle bypass. The positioning and geometry of the bypass inlet were numerically analysed [33], providing the optimum configuration for the maximum improvement of the mass entrainment. However, the reported improvement was 3.8%, which could be considered substantially lower than those of studies in which R134a [29] and methane [30] flows were analysed. On the other hand, the bypass duct in the steam ejector was considered a potential tool for pressure regulation in off- and on-design conditions [34].

A numerical analysis of the bypass ejector with R744 as a working fluid was presented by Bodys et al. [35]. The best bypass duct shape and positioning with respect to the mixing section improvement of the mass entrainment ratio was 37.0% for the lowest tested pressure lift of 4 bar. The aforementioned studies reported a large potential for performance improvement in the case of properly designed bypass ejectors. However, none of the proposed bypass ejectors was examined experimentally because the validation procedures covered only the baseline ejectors. To the best of the authors' knowledge and comprehensive review of the ejector research field [36], an experimental analysis of the R744 bypass ejector is not available in the literature. Moreover, a control strategy for the bypass duct opening has not been investigated.

In this study, experimental analysis of the R744 bypass ejector is presented and supplemented by a full 3-D numerical simulation of selected cases. The research objectives include evaluating the performance of the bypass ejector and developing a control strategy for the bypass duct opening. The ejector geometry with the bypass investigated in the preliminary study [35] was used to manufacture the research construction with stepwise regulation of the bypass duct opening. The prototype was implemented in a laboratory R744 refrigeration unit dedicated for ejector tests. The exchangeable modules of the ejector prototype allowed for the performance mapping of the four bypass positions. The refrigeration conditions of the unit operating in warm and hot climate zones were investigated. Up to 37% of the ejector efficiency improvement in the off-design conditions with low-pressure lift was registered. Regarding supercritical motive conditions, the prototype was numerically studied using the homogeneous equilibrium model (HEM) [37] of the two-phase carbon dioxide flow through the ejector. Consequently, features of the flow with the closed and open bypass ducts were analysed based on the absolute pressure and velocity magnitude distribution. On this basis, the application potential of the bypass ejector was experimentally confirmed along with a proposition for further improvement of this device.

2. R744 laboratory installation dedicated to the ejector performance evaluation

A laboratory R744 refrigeration unit dedicated to ejector tests was used for the experimental analysis of the bypass ejector. An enhanced description and stability analysis of the installation was published by Haida et al. [38]. The test rig, presented in Fig. 1, was designed to cover the motive nozzle capacity at 360 kg·h^{-1}. For this reason, the Dorin CD1400H compressor was selected. The high-side pressure was additionally controlled using the Danfoss CCMT type expansion valve (HPV) operating in parallel with the ejector lines. Hence, the R744 loop was a transcritical booster system with medium-temperature evaporation supported by ejector lines and an internal heat exchanger (IHX). The heat sources were served by auxiliary glycol loops that were connected with an additional heat exchanger. The heat was delivered by six heaters in the glycol tank and by the aforementioned glycol-glycol heat exchanger. All heat exchangers were manufactured by the SWEP company. Finally, the control system was based on the AK-PC-782A Danfoss unit, and all measurements were recorded by Danfoss StoreView software and then by an in-house developed script.

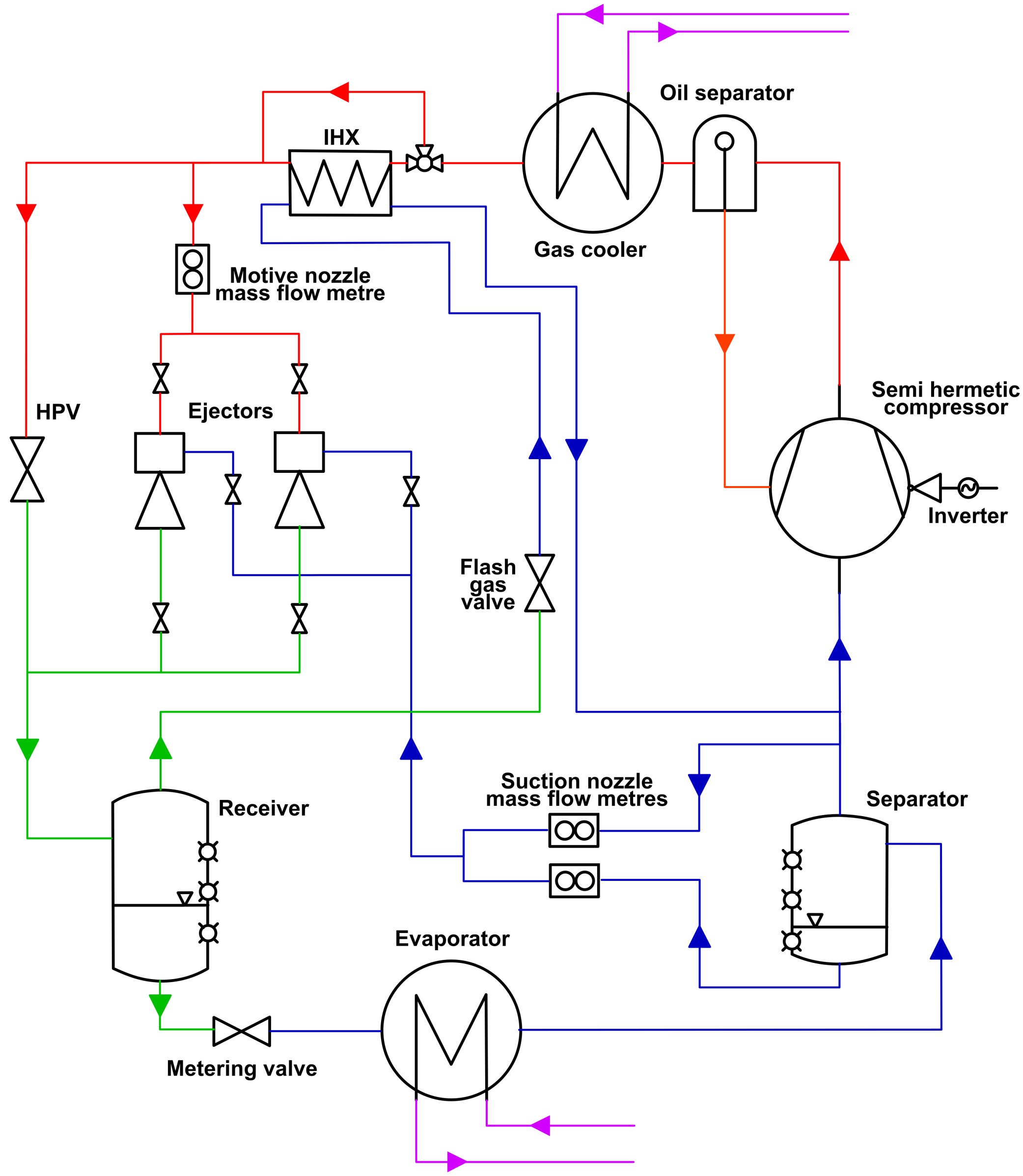

Figure 1: Overall scheme of the laboratory R744 test rig for ejector analysis

The dedicated temperature and pressure sensors were mounted approximately 10 cm from the ejector ports. The location of the sensors is presented in Fig. 2, along with the investigated bypass ejector and the visualisation ejector for other research. Moreover, the motive and suction mass flow rates were measured using Coriolis-type mass flow metres manufactured by Endress+Hauser. The accuracy of the sensors and uncertainty of the output parameters were computed on the basis of NIST guidelines [39] and are listed in Table 1. The steady-state conditions of the considered operating point were assumed on the basis of 10-minute periods with a probing step of 5 seconds and the uncertainty values satisfying the levels listed in Table 1. Consequently, the period contained 120 probes per operating point, which allowed for the reliable evaluation of the ejector operation.

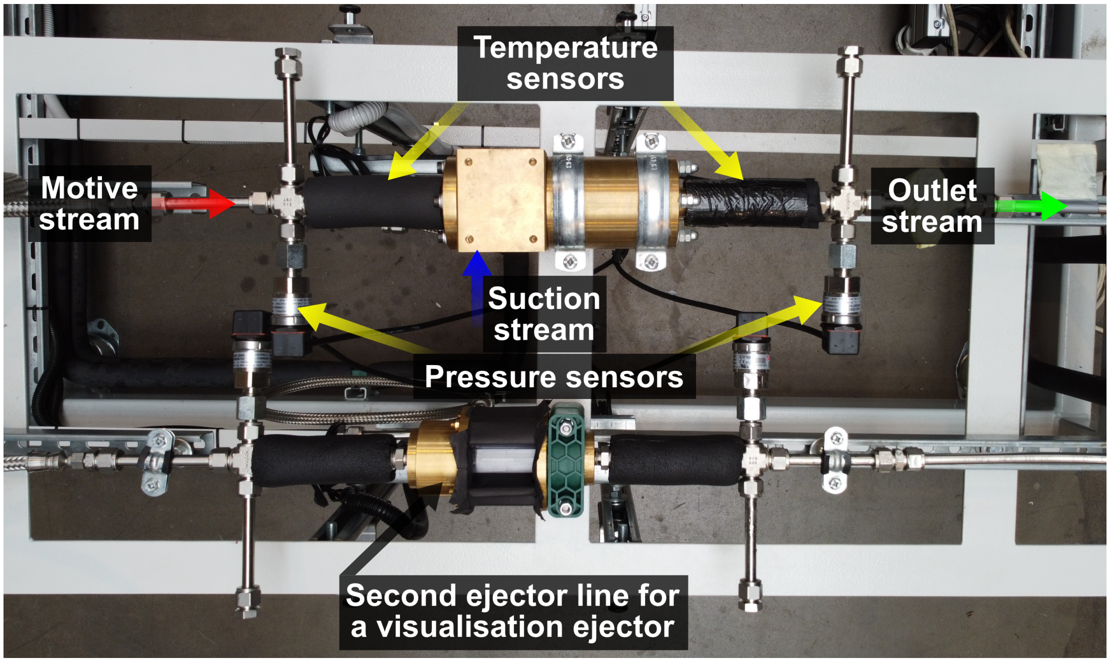

Figure 2: Localisation of the measurement sensors dedicated to the ejector inlet and outlet ports

Table 1: Accuracy and uncertainty of the measured parameters and the computed factors [39]

Parameter	Data source	Accuracy / Uncertainty Type A
Pressure	Danfoss AKS 32R Ratiometric pressure transmitter	±0.3% / ±0.35bar & ±0.15bar (motive & suction)
Temperature	Danfoss AKS-21 PT1000	±(0.3+0.005 · reading) / ±0.05°C
Motive nozzle mass flow rate	Endress+Hauser Coriolis type flowmeter	±0.75% / ±3.0 $kg{\cdot}h^{-1}$
Suction nozzle mass flow rate	Endress+Hauser Coriolis type flowmeter	±0.75% / ±3.0 $kg{\cdot}h^{-1}$
Factor	Formulation	Uncertainty Type C [39]
Efficiency	formulation of Elbel and Hrnjak [18]	±1.0%
Mass Entrainment Ratio	ratio of the suction to the motive mass flow rate	±0.01
Pressure lift	difference between the outlet and the suction port pressure	±0.15 bar

3. Design of the prototype ejector with a suction nozzle bypass

The ejector scheme is presented in Fig. 3, and the dimensions of the motive nozzle are presented in Table 2. The utilised ejector shape with an axial suction nozzle inlet was proposed by Banasiak et al. [40]. In this study, the tangential inlet of the suction nozzle was used. Namely, the ejector was dedicated for transcritical operation of the system located in warm climate (approximately 36°C of ambient temperature) with evaporation temperatures at the level of -6°C and pressure-lift conditions at the level of 8 bar (i.e. corresponding temperature level demanded for air-conditioning). The geometry of the bypass duct and its positioning are described separately in subsections 3.1 and 3.2 for the sake of scheme clarity. Brass was used for the entire construction of the ejector ducts. The manufacturing tolerances were in the ranges of ±0.01 mm, ±0.05 mm and $\pm 0°3'$ for the diameters, lengths and angles, respectively. The roughness of the internal surfaces was Ra=0.5. The entire construction was assembled using independent parts for the motive nozzle, the suction chamber, the mixing chamber, the movable diffuser and the outlet port. This means that the prototype is based on several exchangeable pairs of movable diffuser and mixing chambers, which allows for the analysis of the various bypass positionings.

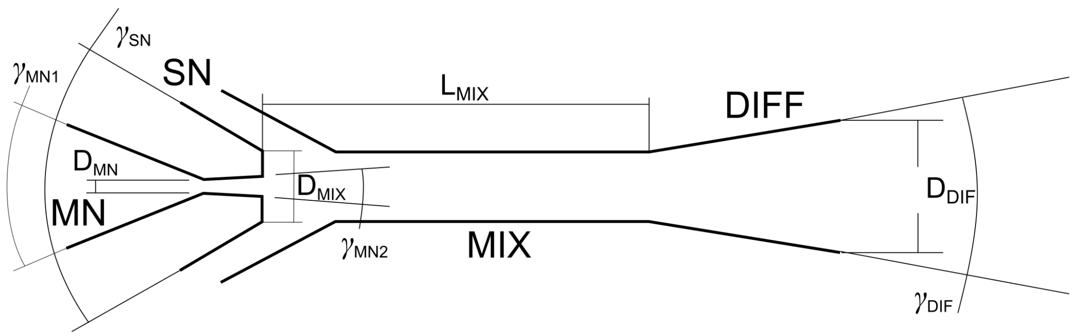

Figure 3: General scheme for a standard ejector geometry: motive nozzle (MN) section, suction nozzle (SN) section, mixing (MIX) section and diffuser (DIFF) section

Table 2: Geometrical parameters of the tested ejector motive nozzle

Parameter name (symbol)	Unit	Value
Throat diameter (D_{MN})	mm	1.4
Converging angle ($\gamma_{MN,1}$)	°	30.0
Diverging angle ($\gamma_{MN,2}$)	°	2.0
Suction angle (γ_{SN})	°	38.0
Mixing diameter (D_{MIX})	mm	6.0
Mixing length (L_{MIX})	mm	16.0
Diffuser diameter (D_{DIF})	mm	8.4
Diffuser angle (γ_{DIF})	°	5.0

3.1. Opening and closing mechanism of the bypass duct

According to the bypass regulation concept presented in [35], one tangential suction port delivers R744 into two chambers: the standard one for the suction nozzle and the additional one for the bypass nozzle. The flow between these chambers is controlled by the bypass opening procedure. Hence, the bypass opening mechanism is located inside the ejector walls, as presented in Fig. 4 in the 2-D scheme (top) and 3-D view (bottom). Namely, the diffuser part (B2) is strictly correlated with the mixer part (B1) to provide the positioning and shape of the bypass duct. The properly designed regulation screws hold the diffuser part (B2) in the closed position. The opening is based on the translation of the diffuser part (B2). To open the bypass duct, the screws need to be loosened, which results in translation of the diffuser part (B2). The translation is provided on the basis of the pressure difference between the suction chamber and ambient environment. A closing procedure is realised in the opposite way where the screws need to push the diffuser part. Both procedures have to be realised manually, which takes up to 5 seconds. Finally, the opening/closing of the bypass is conducted during the installation operation. Hence, the effect of the bypass opening/closing is recorded *online* and in a continuous way for the same set of operating conditions.

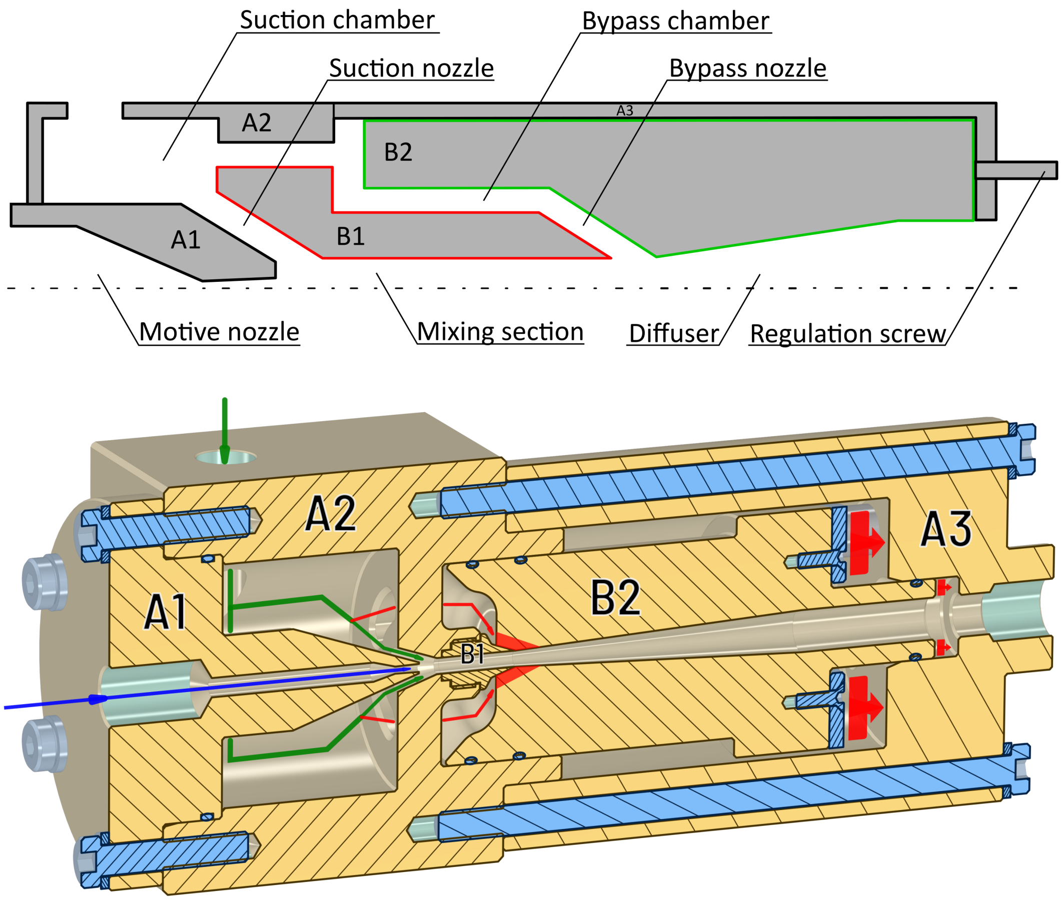

Figure 4: Cross section of the bypass ejector with stationary parts (A1, A2, A3 and B1) and a movable diffuser part (B2) using the 2-D scheme (top) and 3-D view (bottom)

3.2. *Positioning of the bypass duct*

A change in the bypass position along the ejector axis involves more time than the opening/closing procedure because it requires stoppage of the installation. Then, the ejector line is closed, and a pair of mixer and diffuser parts needs to be exchanged. In the last step, the ejector line is vacuumed and refiled before further tests. The pairs of mixing and diffuser sections were designed on the basis of numerical assessment of the bypass ejector [35]. The connection point of the parts indicates the location of the bypass duct along the ejector axis. The scheme of the investigated bypass duct geometry is presented in Fig. 5 The angle β_{bps} was 19°, while the bypass nozzle width d_{bps} was 1.6 mm. The shape of the bypass nozzle was adapted strictly from the preliminary 2D numerical analysis [35]. The conclusions from this preliminary analysis showed that the bypass nozzle shape was less important than the positioning of the bypass duct. Hence, the shape from the preliminary analysis was used in this study.

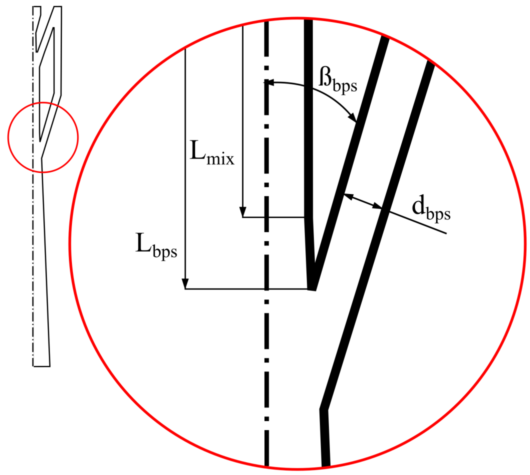

Figure 5: Scheme of the bypass duct with characteristic geometrical parameters

In general, the bypass duct takes the role of the second suction nozzle and has the same dimensions as the baseline suction nozzle based on the previous numerical assessment of the R744 bypass ejector performance [35]. The positioning of the bypass duct along the ejector axis was defined as follows:

$$\Psi = L_{bps}/L_{mix} \tag{1}$$

where Ψ represents the dimensionless position of the bypass duct along the ejector axis–for clarity, this nomenclature will be used in this study. L_{mix} is the length of the constant-area mixing section that was constant for the tested positions, and L_{bps} is the length along the ejector axis from the beginning of the constant-area mixing section to the location of the bypass nozzle introduction. Four pairs of mixing and diffuser parts were manufactured to investigate Ψ equal to 1.0, 1.1, 1.2 and 1.3. Hence, Ψ=1.0 indicates the bypass nozzle at the mixer and diffuser connection. A higher value of Ψ indicates that the bypass nozzle is introduced farther into the diffuser. The distance between each position is approximately 1.6 mm.

4. Methodology of the experimental evaluation of the bypass ejector performance

The investigated range of the motive nozzle conditions was based on the operating curve of the motive nozzle port defined by Gullo et al. [41] for the R744 refrigeration system equipped with a multi-ejector in a warm climate condition, such as a Mediterranean climate. Three operating conditions for the motive nozzle were used, as illustrated in Fig. 6, in groups A, B and C. The groups were represented by absolute pressure levels of 81 bar, 86 bar and 91 bar and corresponding temperatures of 33°C, 36°C and 39°C. Regarding the aforementioned operating curve dedicated to the refrigeration conditions, the pressure level of the suction nozzle port was chosen using typical refrigeration conditions, such as those of chillers. Hence, saturation pressures for evaporation temperatures of -10°C and -6°C were tested. The suction temperature was controlled at 0°C and 4°C for the lower and higher evaporation temperatures, respectively. Each pair of motive and suction conditions was tested with 5 levels of pressure lift from 4 bar to 11 bar. The range of the pressure lift was correlated with the criterion of steady-state ejector operation, and the aim of this study focused on the bypass application potential. Namely, transcritical booster R744 systems, such as those of local retail points or the food processing industry, should be applied.

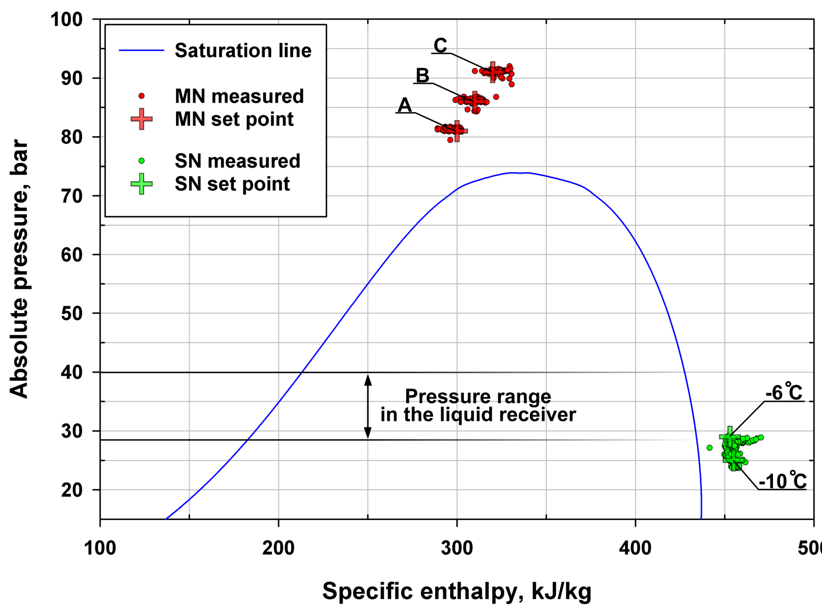

Figure 6: Investigated motive nozzle and suction nozzle conditions on the p-h diagram of R744

The aim of the study was to evaluate the performance of an ejector equipped with a bypass duct compared to that of a standard ejector. Nevertheless, some variations in the operating conditions occurred, as presented in Fig. 6. The following measurement procedure was used to provide maximum similarity of the operating conditions during the comparison of ejector performances with open and closed bypass ducts. Namely, the tests for each point were started by an assembly of the proper bypass position in the ejector line. Next, a pair of motive conditions and evaporation temperatures was selected. Stabilisation of the test rig thermal conditions required approximately one hour. Finally, the measurement procedure for the given steady-state conditions was as follows:

1. Measurement of the ejector performance with a **closed bypass duct**
2. Bypass duct opening
3. Measurement of the ejector performance with an **open bypass duct**
4. Bypass duct closing

5. Increase in the pressure lift for the next measurement point

Consequently, each operating point with open bypass possessed an individual corresponding point with standard ejector operation for reliable comparison. Hence, the proposed procedure allowed for the evaluation of the ejector performance based on the efficiency formulation described by Elbel and Hrnjak [18]. The efficiency is defined using the absolute pressure, temperature and mass flow rates as follows:

$$\eta_{ej} = \frac{\dot{W}_{rec}}{\dot{W}_{rec,max}} = \chi \cdot \frac{h(p_{OUT}, s_{SN}) - h(p_{SN}, s_{SN})}{h(p_{MN}, s_{MN}) - h(p_{OUT}, s_{MN})} \tag{2}$$

where η_{ej} is the ejector efficiency, χ is the mass entrainment ratio, $\dot{W}$ is the expansion work rate, s is the specific entropy and the subscript OUT denotes the ejector outlet. The formulation represents an expansion work rate recovered (subscript rec) by the ejector with respect to the maximum possible expansion work rate recovery potential (subscript rec, max).

5. Modelling approach for the numerical evaluation of the bypass ejector

The CFD techniques allowed for the analysis of the 3-D flow behaviour in the prototype bypass ejector. The numerical analysis was focused on the R744 flow evaluation in the suction chambers what was not possible to realise on the basis of experimental tests. Consequently, a discussion of potential further improvements of the device was possible. The simulation of the two-phase carbon dioxide flow through the bypass ejector was based on the data delivered from the dedicated laboratory test rig discussed in Section 2. Hence, a direct validation process of the model output was provided. Moreover, the numerical domain contained ducts up to the location of the pressure sensors (see Fig. 2). This means that the pressure drop between the measurement point and the ejector ports was included in the computational model.

5.1. Approach for the two-phase transonic simulation of the R744 flow

The two-phase flow simulation was based on the HEM presented in [37]. This approach assumes thermodynamic and mechanical equilibrium between the two phases flowing through the ejector ducts. Moreover, an instantaneous evaporation process is assumed during the expansion process in the motive nozzle. Regarding the range of operating conditions at the ejector motive port, this approach was extensively validated, resulting in a high motive nozzle mass flow prediction accuracy of 10% [42]. The accuracy of the suction nozzle mass flow rate prediction was validated at 15% of the relative error [42]. In this study, the computed mass flow rates at the motive and suction ports were validated against data from the laboratory test rig.

5.2. Computational procedure

The 3-D domain of the prototype ejector was generated. The computational platform *ejectorPL* described in the work of [42] generated numerical grids characterised by negligible influence on the numerical solution. In this study, the same numerical grids were used for the main flow ducts of the ejector. The additional inlet ducts, suction and bypass chambers were generated separately and connected with the ejector. According to Section 2, the absolute pressure and temperature measured in closure of each ejector port were used as the boundary condition of the computational procedure. The simulation process was assumed to be finished when the relative residuals of each equation were below 10^{-4}, and the mass imbalance was lower than 0.1% of the suction nozzle mass flow rate. The total mass flow rate at each ejector port was compared to the measured values, and relative errors were computed as follows:

$$\delta_m = \frac{m_{SIM} - m_{EXP}}{m_{EXP}} \cdot 100\% \tag{3}$$

where δ_m is the relative error of the mass flow rate data obtained using the CFD model (subscript SIM) compared with the experimental (subscript EXP) data.

6. Results and discussion

6.1. Bypass positioning and performance improvement

In the experimental procedure, the tested ejector with the specified Ψ was exposed to all the operating conditions, while the tests of the closed and open bypass ducts were realised successively, as discussed in Section 4. Hence, the variation in the ejector performance with the closed and open bypass ducts could be described as a relative difference in the ejector efficiency, as presented in Fig. 7, for each of the four investigated Ψ values. The only variation between the operating conditions measured with closed and open bypass duct were due to natural instabilities of the control unit handling with the thermal inertia of the installation. However those instabilities were maintained below the level described in the Table 1 hence it could be evaluated as a negligible from the point of view of the ejector efficiency. The relative difference of the efficiency presented in Fig. 7 is affected in vast majority by the change of the mass entrainment ratio, specifically by the change of the suction nozzle mass flow rate. However, despite that the authors decided to use efficiency values in order to include those minimal variations of the operating conditions regarding full reliability of the results. In Fig. 7 series were marked according to the evaporation temperature, where -6°C and -10°C were described by circles and triangles, respectively. The conditions at the motive nozzle inlet are represented in Fig. 6 by the letters A (85 bar and 33°C), B (86 bar and 36°C) and C (91 bar and 39°C) and additionally by the colours blue, green and red, respectively. Additionally, the pair of cases (Ψ=1.1) considered further in the numerical analysis in Section 7 is marked by a green dashed ring. These cases are selected on the basis of positioning analysis below and will be use to evaluate the R744 flow in the suction chambers which could not be done by experimental test.

A previous study showed that the implementation of the bypass duct into the R744 ejector achieved the most success in the case of the choked mixing section during unfavourable off-design operating conditions [35]. In this study, experimental tests confirmed this statement. Namely, the higher the motive nozzle conditions were, the more improvement of the ejector efficiency could be obtained after the bypass opening. This is indicated by red-coloured markers positioned higher than green-coloured markers. Simultaneously, the lower the suction pressure reflected by the evaporation temperature was, the more improvement was available for the tested bypass ejector compared to the standard design. Hence, the circular markers (evaporation temperature set to -6°C) indicate lower values than the corresponding triangular markers (evaporation temperature set to -10°C). Second, considering the outlet port conditions, the pressure lift was an investigated parameter. Namely, the improvement level of the ejector performance was reduced with the increasing pressure lift value in all the tested Ψ. This relationship could be described as almost linear. Unfortunately the range of the pressure lift with potential benefits of the bypass utilisation could be evaluated as a narrow in the case of the evaporation temperature set to -6°C. Wider range (looking at the pressure lift value) was obtained in the case of $T_0 = -10°C$. The ejector efficiency improvement was observed for a maximum pressure lift of almost 7.5 bar (Ψ=1.1), which should be considered a perspective for further development of the bypass ejector. Namely, compared to the preliminary numerical evaluation of the bypass idea, the efficiency of the ejector after bypass opening could be improved only for a pressure lift of 4 bar [35].

The obtained efficiency improvement was correlated with Ψ in a more significant way than that presented in the preliminary numerical analysis [35]. The highest efficiency increment was indicated with Ψ=1.1, when an improvement of 5% for the pressure lift of 7 bar was obtained under the operating conditions of the motive conditions from group C and a lower evaporation temperature. Reducing the pressure lift to 5 bar allowed for 34% of the efficiency improvement. Under the motive nozzle conditions from group A and an evaporation temperature of -10°C, it was challenging to obtain steady operation with the lower pressure lift values for which even higher improvements are expected. The reasons were related to the unstable regulation of the metering valve and consequent fluctuation of the suction mass flow rate. For Ψ=1.2, the maximum pressure lift correlated with the performance increment was reported at 6.5 bar. However, the lowest pressure lifts allowed for an 8 percentage points lower relative difference than in the case of Ψ=1.1. The maximum reported improvement was 37% in the case of Ψ=1.3 for a pressure lift of 5 bar. Nevertheless, the latter position did not result in improved ejector operation with a pressure lift higher than 6 bar. The bypass positioned directly at the connection of the mixing section and diffuser (Ψ=1.0) provided the lowest improvement values of approx. 10%, demanding additionally even lower pressure lifts.

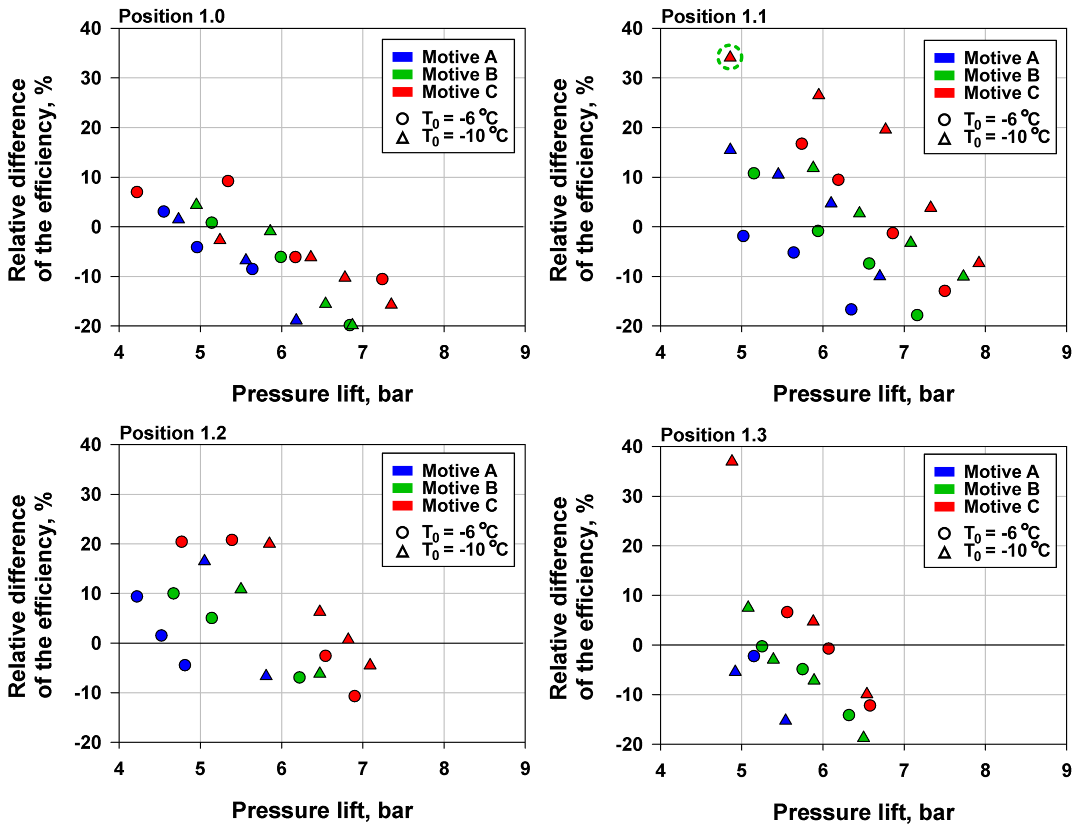

Figure 7: Relative difference in the ejector efficiency for four bypass opening positions (the case analysed numerically is indicated by a green ring)

6.2. *Efficiency of the ejector with proper control of the bypass duct opening*

This subsection presents the efficiency characteristics of the bypass ejector, including proper control of the bypass duct opening. The measurement results obtained for the higher suction and lower suction pressures are presented in Fig. 8 and Fig. 9, respectively. The cases in which the bypass duct should be closed for higher efficiency are marked by crosses. Situations in which the bypass duct should be open are marked by circles (for higher suction pressure) and triangles (for lower suction pressure). Similar to Fig. 7, the motive nozzle conditions were organised by blue (A), green (B) and red (C) colours according to the increasing pressure and temperature values. These results were divided into four graphs corresponding to Ψ.

The control strategy of the bypass duct opening should be aimed at the highest possible ejector efficiency. Consequently, the efficiency of the bypass ejector is higher than that of the standard design in the area of the lower pressure lifts. Considering the standard ejector efficiency, this factor takes the lowest values at the aforementioned low-pressure lift operation. Lifting the efficiency in this region provides a substantially flatter character to the efficiency distribution with varying pressure lift values. For an evaporation temperature of -6°C, the minimum registered efficiency was increased from 18.5% to 19.8%. However, when the suction pressure corresponded to a saturation pressure of -10°C, the minimum registered efficiency was improved more substantially from 14.4% to 19.3%. Moreover, in addition to the improved efficiency, more stability of the ejector performance was a benefit of the bypass introduction. Namely, considering all measurement points with the evaporation temperature set to -6°C, the average bypass ejector efficiency with a properly controlled opening was 28.4% with a standard deviation of 2.2 percentage point. The measurement results at the lower suction pressure provided an average bypass ejector efficiency of 26.6% with a standard deviation of 1.8 percentage point. Finally, the introduced bypass raised the efficiencies in those regions which were out of the design conditions – from the point of view of the pressure lift. Consequently, the prototype ejector could cover a wider range of operating conditions with high and more uniform efficiency values than those of the standard construction.

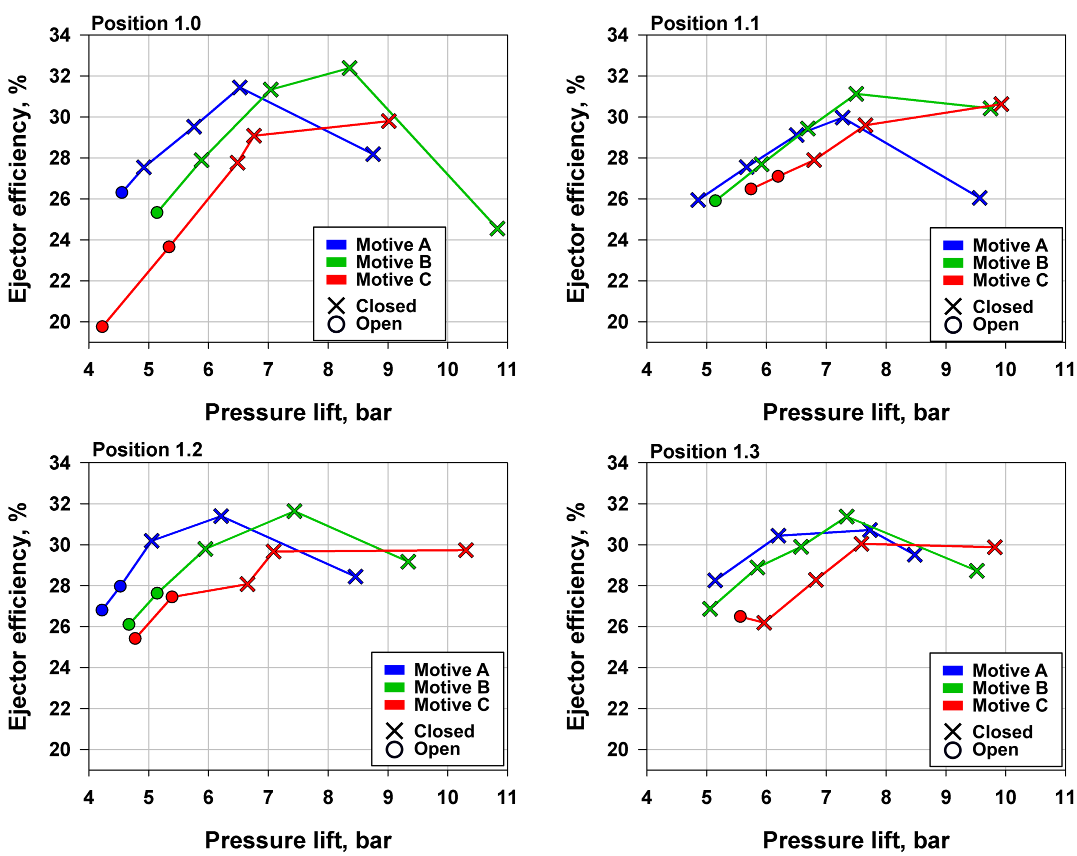

Figure 8: Compilation of the highest ejector efficiency with proper opening of the bypass at an evaporation temperature set to -6°C for four bypass opening positions

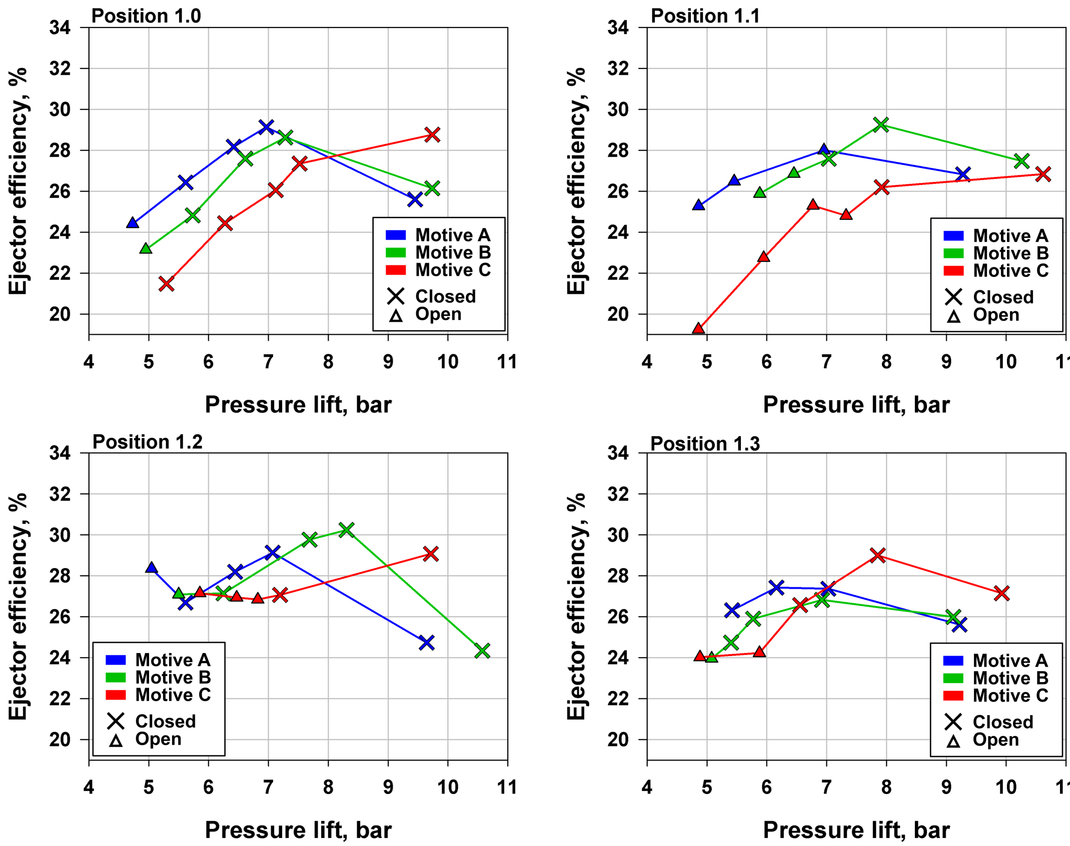

Figure 9: Compilation of the highest ejector efficiency with proper opening of the bypass at an evaporation temperature set to -10°C for four bypass opening positions

6.3. *Influence of the motive and suction temperatures on the bypass performance*

An analysis of the R744 temperature influence on the bypass potential was provided for the motive and suction ports separately. The aim was to check the sensitivity and then the potential instabilities in the ejector work in function of the motive and the suction temperatures which would be delivered by the various thermal states of the system, especially variable conditions of the heat rejection in the gas cooler and different heat load of the evaporator. For each port, three temperature levels were investigated, while other operating conditions were maintained at the same level, as presented in Table 3. Two positions of the bypass opening resulted in six operating points per motive and suction port analysis. The motive port analysis was performed at 29°C, 33°C and 37°C and a pressure lift of 4.5 bar. The influence of the temperature at the suction port on ejector performance was assumed to be less significant. Hence, a pressure lift of 6.0 bar (higher efficiency) was used to clearly present the influence of the suction temperature. Moreover, a higher step of 8 K between the points was used starting from the suction temperature of 9°C. The suction temperatures provide deterioration of the R744 refrigeration system coefficient of performance; however, they were used to evaluate its influence on the bypass ejector.

Table 3: Operating conditions for the ejector efficiency analysis at different motive and suction nozzle temperatures

No.	Bypass	Motive conditions		Suction conditions		Outlet conditions	
		bar	°C	bar	°C	bar	°C
M1	closed	90.6	**29.6**	28.1	18.5	32.4	-1.3
	open	90.9	**28.8**	27.9	19.0	32.6	-1.0
M2	closed	91.0	**33.7**	28.0	18.3	32.8	-0.7
	open	91.2	**33.9**	27.9	18.7	33.0	-0.4
M3	closed	91.3	**37.5**	28.1	20.1	32.8	-0.7
	open	91.1	**37.6**	27.9	20.5	33.1	-0.2
S1	closed	91.0	38.3	28.0	**9.6**	34.0	0.5
	open	91.2	38.6	28.0	**8.8**	34.2	0.8
S2	closed	91.2	38.7	28.2	**16.6**	34.1	0.7
	open	91.2	39.1	28.2	**16.9**	34.2	0.8
S3	closed	90.9	37.9	28.2	**24.1**	34.1	0.9
	open	91.1	37.9	28.3	**25.3**	34.1	0.8

The output of the R744 temperature analysis is presented in Fig. 10 for the motive nozzle (left graph) and for the suction nozzle (right graph). The ejector efficiency values with closed (black bars) and open (red bars) were compared using relative differences (green bars). The motive nozzle analysis revealed similar efficiency improvements for M1 and M2. Moreover, the bypass ejector efficiency increased from M2 to M3, while the standard ejector design obtained efficiency (black bars) at 20.0%. The influence of the motive nozzle was substantial, as presented in the aforementioned analysis and in Fig. 7. However, the improvement potential of the bypass ejector was at constant and high levels despite the changes in the motive nozzle temperature. Consequently, the aforementioned similarity between the efficiency at conditions M2 and M3 provided information that starting from approximately 33°C the ejector operates with the uniform efficiency at the level of 20% despite unfavourable low pressure-lift value at the level of 4 bar. On the other hand, this region of the operating conditions could be improved in the most significant manner what was represented by the highest green bar indicating over 30% of the relative difference of ejector efficiency comparing closed and opened bypass.

The analysis of the suction nozzle temperature presented in the rightward graph of Fig. 10 showed the moderate importance of this parameter. The opening of the bypass duct resulted in a similar improvement of approx. 8.5% at lower suction temperatures S1 and S2. The highest suction temperature resulted in a lowered (-7.0%) efficiency of the bypass ejector. Nevertheless, despite large temperature increments, the ejector performance remained in the range of 26.0% to 28.0%. Consequently, the influence of the suction temperature should be considered negligible because of the similar prototype and standard design efficiencies in all examined cases.

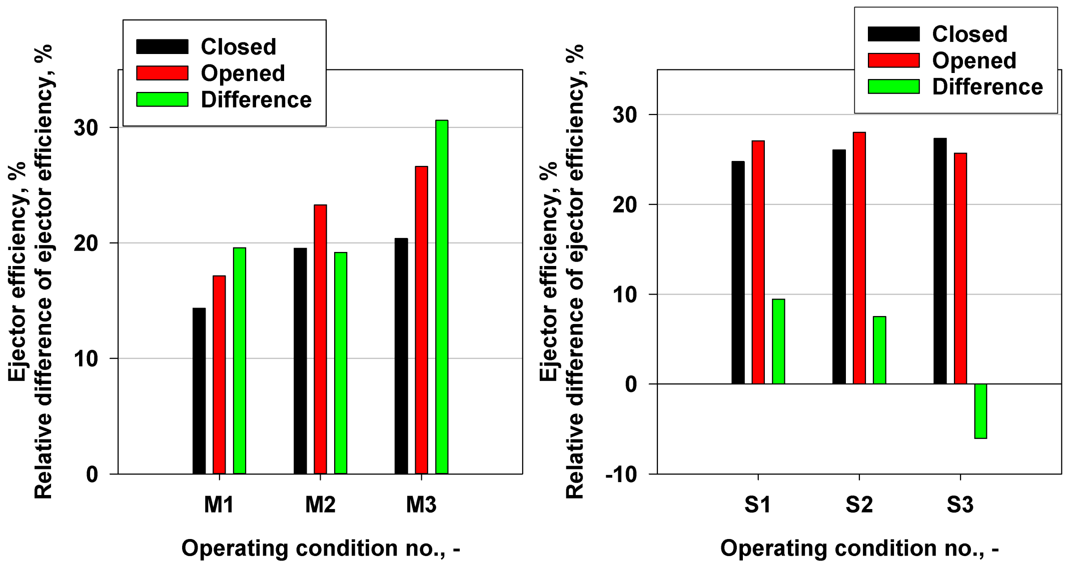

Figure 10: Influence of the motive nozzle temperature (left) and the suction nozzle temperature (right) on closed (black bars) and open (red bars) bypass ducts and the resulting relative difference (green bars)

6.4. Analysis of the opening degree of the bypass duct

The effect of the bypass opening degree on ejector performance was investigated for Ψ=1.1. The opening degree of the bypass duct in the prototype ejector can undergo stepless modulation from 0.0% to 100.0% and was formulated as the ratio of actual Part B translation (see Fig. 4) to the maximum translation of 5.0 mm. For this analysis, operating condition C-10 and a pressure lift of 5.0 bar were selected. Hence, it provided the maximum improvement for the selected bypass position.

The results obtained from the opening degree analysis are presented in Fig. 11. The results showed that full available improvement for each case was obtained with approximately 7.0% to 10.0% of the opening degree. In this opening, the width of the bypass nozzle d_{bps} was approximately 0.16 mm (see Fig. 5). It might be interpreted that the influence of the pressure introduced at the beginning of the diffuser could be a crucial factor behind the bypass improvement. Resulting mixing pressure was increased and provided reduction of the choked mixer phenomenon (further discussed in Section 7.3 and Fig 12). It could be stated that the aforementioned width of the bypass duct at 10.0% of the opening was large enough to provide losses-free flow through this secondary bypass nozzle. On the other hand, this could be a consequence of the fact that this opening was sufficiently large to provide a full available suction stream through the bypass duct. Moreover, in this situation, the ratio of the suction nozzle and bypass duct mass flow rates should be considered a high value because of the low value of the latter component. Hence, the geometry of the suction nozzle and the mixer chamber could still be described as a substantial design feature for the ejector performance even in the case of bypass duct utilisation. The measurement points of the higher opening degree were characterised by variations of ±1.5% of the ejector efficiency, which should be related rather to the variations of the operating conditions. Finally, in the analysed ejector design, a large buffer is available for the additional suction stream flow through the bypass duct at evaporation temperatures lower than the investigated values.

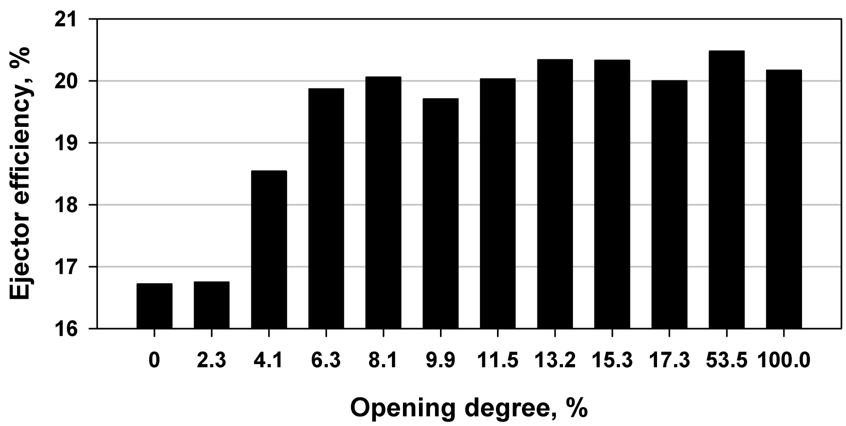

Figure 11: Ejector efficiency for different opening degrees of the bypass duct

7. Numerical analysis of the ejector operation with closed and open bypass ducts

7.1. Validation results

The numerical analysis in this study aimed for the evaluation of the R744 flow in the suction chambers of the prototype ejector. For this purpose only one operating condition was required hence this was a range of necessary validation process. Namely, two cases for that operating condition were validated – one case with open and one case with closed bypass duct. The performance of the suction chambers during the ejector operation with open and closed bypasses was numerically analysed for the best case from Ψ=1.1. The analysis would reveal a potential for further improvement of the suction phenomena in the case of already high increment of the ejector efficiency. Namely, the lowest pressure lift in operating condition C-10 was selected (marked by the green ring in Fig. 7) for the numerical analysis provided in this Section.

First, the main output data from the simulation were validated against the experimental data from the test rig, as presented in Table 4. Regarding the simulation of the closed bypass scenario, the accuracy of the mass flow rate predictions (as defined in Eq. 5.2) was -2.3% and 11.3% for the motive and suction ports, respectively. In the case of the open bypass duct, the aforementioned accuracy was slightly higher. In both cases, the stream at the suction port was overpredicted, and the level of these inaccuracies was similar. Hence, the validation results were considered sufficiently good for further analysis in which the ejector operations with the open and closed bypasses were compared.

Table 4: Validation data of the ejector simulation and results of the suction stream analysis

Validation parameter		Bypass closed	Bypass open
Motive port	simulation, kg/s	0.0695	0.0691
	experiment, kg/s	0.0712	0.0695
	δ_m, %	-2.3	-0.6
Suction port	simulation, kg/s	0.0318	0.0362
	experiment, kg/s	0.0286	0.0337
	δ_m, %	11.3	7.3

7.2. *Analysis of the suction stream distribution*

The results of the analysis based on the suction stream distribution between the suction nozzle and the bypass nozzle are presented in Table 5. Such data could not be obtained from the laboratory test rig due to the closed construction of the ejector. Hence, measurement of the mass flow rate is available only for the total suction stream. A substantial amount of the total sucked R744 was directed to the suction nozzle. The bypassed stream was on the level of approximately 15.0% of the total suction stream computed at the suction port. The low ratio between the bypassed and total suction streams could be found as a reflection of the data presented during the opening degree analysis in which a small opening (see Fig. 11) was sufficient for a full improvement of the ejector performance. Moreover, the simulation showed that the change in the suction nozzle mass flow rate was equal to -3.6%, which is negligible compared the cases with closed and open bypass duct operations. Hence, the vast majority of the additional R744 sucked after the bypass opening was directed to the bypass nozzle. Namely, the overall change in the suction stream was 13.9% in the case of the simulation output, while a slightly higher (by 4.3% percentage points) change was measured at the test rig.

Table 5: Results of the suction stream analysis

Parameter		Value
Simulation	suction nozzle, kg/s	0.0306
	bypass nozzle, kg/s	0.0056
	suction nozzle / total suction stream, %	84.6
	bypass nozzle / total suction stream, %	15.4
	suction nozzle stream change, %	-3.6
	total suction stream change, %	13.9
Experimental	total suction stream change, %	18.2

7.3. *Discussion of the possible further shape improvements of the bypass ducts*

The absolute pressure distribution in the ejector was obtained from the numerical simulation for both variants. These results are presented in Fig. 12 in the form of the cross-sectional field (top) and the corresponding distribution along the ejector axis (bottom). The maximum value at the field range and vertical axis of the graph was set to 3.0 MPa to clearly illustrate the absolute pressure distribution in the mixer region.

Cross-section A indicates the beginning of the mixing section where choked flow and Prandtl-Meyer shock-train flow are visible. The bypass opening resulted in increased absolute pressure in the aforementioned region. In the case of the field data, the near-wall region at the beginning of the mixer changed colour from azure to green, i.e., by approximately 0.55 MPa. The pressure profiles in this region differ by 0.17 MPa. Considering the ejector axis, the pressure difference is higher at the end of the mixing section marked by cross-section B (0.44 MPa) and at the beginning of the bypass chamber indicated by cross-section C. Cross-section D indicates a uniform pressure distribution across the duct and the same pressure values in the ejector axis for both cases. The pressure distribution in the diffuser is similar; however, the red circles of the open bypass case are located slightly higher than the markers of the closed bypass. The absolute pressure is identical at the bypass nozzle and suction nozzle inlets as indicated by the yellow colour in both areas. Consequently, the channel that connects these regions provides a negligible pressure drop. Finally, the mechanism of ejector unchoking could be related to the flattened pressure profile and higher pressure level at the end of the mixing section after bypass duct opening.

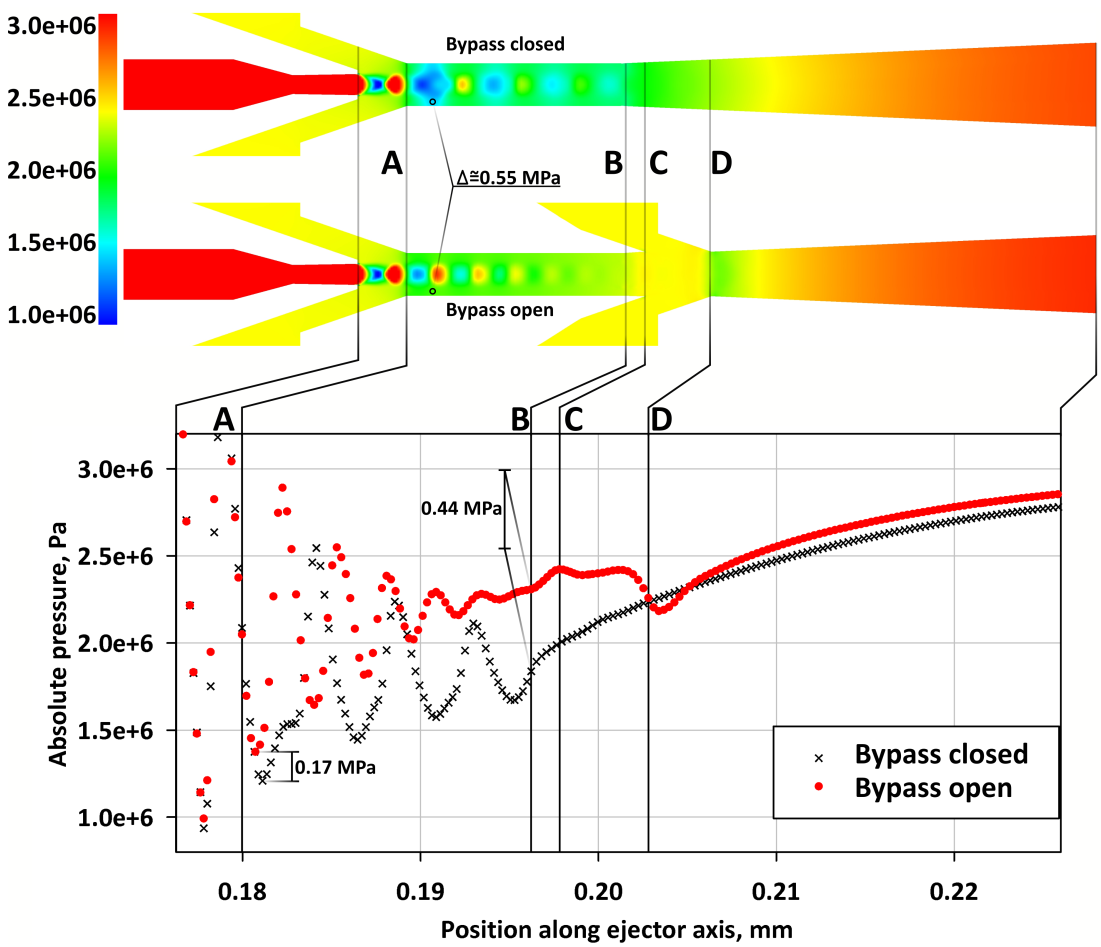

Figure 12: Comparison of the absolute pressure (Pa) fields (top) and profiles (bottom) of the ejector operation with the closed (black crosses) and open (red circles) bypass ducts

Additional analysis of the suction ducts is provided based on Fig. 13. Fig. 13 contains a composition of the three planes (schematically presented on the right-hand side) with velocity magnitude contours and path lines. In this figure, the velocity range was reduced to 20 m/s to analyse the behaviour of the flow in the suction chamber and the bypass chamber. Two of the planes (top) were placed across ducts that connect the suction and the bypass chamber. The third plane was rotated by 45°(bottom). The velocity magnitude in the suction chamber is 15 m/s, while significantly slower flow was observed in the bypass chamber. The path lines in the suction chamber show uniform swirling flow around the ejector axis. The strong vortex and long pathlines from the suction port to the suction nozzle were a result of the bypass duct design. Namely, the radius of the suction chamber was enlarged (comparing to standard construction) in order to contain the opening mechanism (moving cylinder correlated with proper mixing part, please see Fig. 4) and the ducts which connect the suction chamber and the bypass chamber. Scheme located on the right-hand side of the Fig. 13 presents a cross-section view of the aforementioned connecting ducts (4 shapes similar to a cashew nut). These ducts needed to be located around the part which provided mixing zone hence it was at the larger diameter. This enlargement resulted in the final diameter of the suction chamber. On the other hand, flow in the bypass chamber is more turbulent, and rotational movement around the ejector axis is substantially less visible. Moreover, the distance for effective acceleration of the fluid should be longer in the case of the bypass nozzle. The resulting distribution (see Table 5) of the sucked R744 could be affected by the described differences between the flow in the suction and bypass chambers. The aforementioned differences in the flow pattern in the suction and bypass chambers could be correlated with the cross-sectional shapes of the inlet ducts that connect both chambers. Finally, the introduction of additional swirl motion in the bypass chamber could bring further improvement.

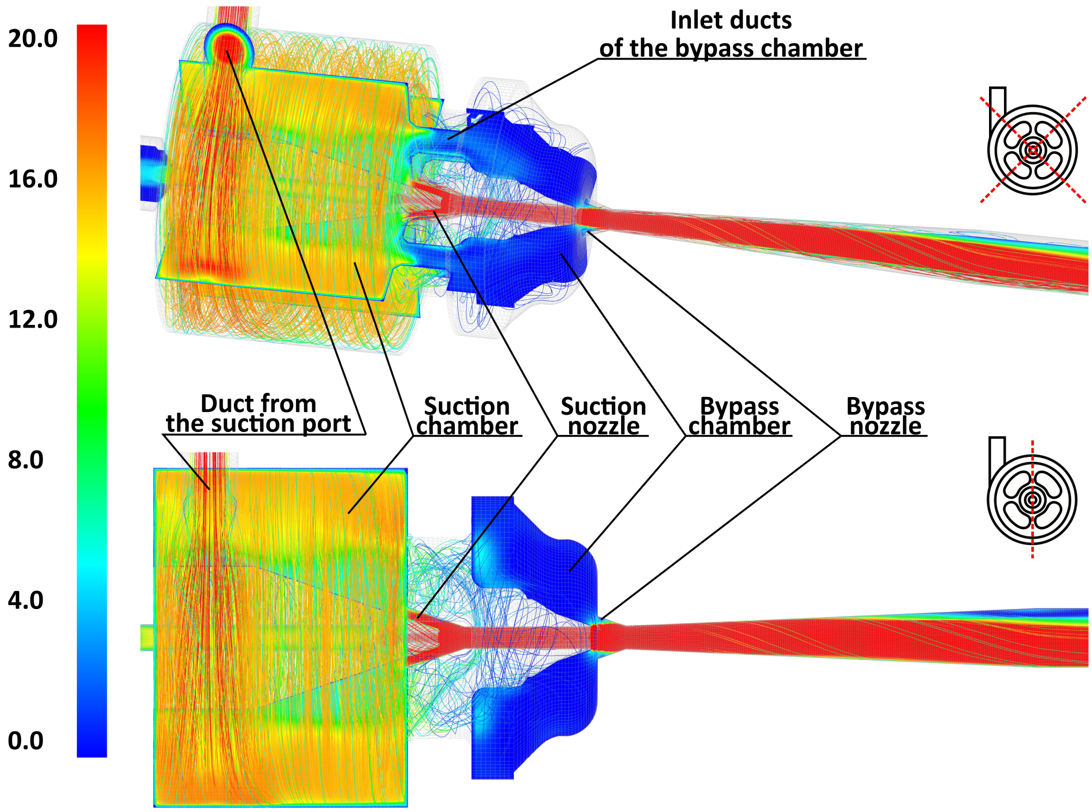

Figure 13: Distribution of the velocity magnitude (m/s) and path lines of the velocity magnitude (m/s) in the suction and bypass chambers in isometric view (top) and side view (bottom)

8. Conclusions and further work

The prototype R744 ejector with the bypass duct of the suction nozzle was designed and manufactured based on baseline ejector design prepared for high-pressure lift conditions. Experimental investigation at a dedicated R744 lab installation was conducted for four bypass nozzle positions along the ejector axis and variable opening degrees. Three sets of high-pressure side conditions characteristic of warm climates were used along with two evaporation temperatures correlated with chilling and refrigeration conditions.

The improvement of the ejector efficiency after the bypass opening was strong and almost linear as a function of the pressure lift. The bypass position described by Ψ=1.1 was evaluated as the best case in the investigated range. The ejector with the bypass duct open in Ψ=1.1 obtained an efficiency improvement for the pressure lift of up to 7 bar. The maximum measured efficiency increment was 37%. The ejector performance was improved in the off-design conditions characterised by the low-pressure lift values and the lowest level of the baseline efficiency. Consequently, the efficiency curve presented higher and more uniform values in a full range of ejector operations. Regarding mobile or integrated HVAC&R applications in which high variation of the cooling load is expected, the bypass ejector should reduce instabilities as a result of a more uniform performance in less favourable operating conditions. Moreover, manufacturing one ejector for a wide range of pressure lift operations could bring economic advantages over two different ejectors designed for low- and high-pressure lift operating ranges.

The pressure and temperature conditions at the motive port of the bypass ejector were more influential than the suction conditions. This feature should be considered an advantage of the examined idea, considering that R744 systems are standard applications in warmer climates. Moreover, the results showed that the application of the bypass ejector should not be affected by the suction temperature. From the point of view of the ejector, this temperature is usually correlated with the temperature after the cooling load component.

The bypass duct in the prototype ejector allowed for the fluent regulation of the bypass opening. The mechanism used the pressure difference between the suction port and ambient environment. Approximately 10% of the opening degree allowed for the full available improvement of the ejector efficiency at the considered operating point. The importance of the bypass suction chamber length was evaluated as less significant because further opening did not influence the ejector performance. Full available improvement after the bypass opening required a small range of part B (see Fig. 4) translation of only 0.5 mm. The mechanism of bypass duct opening should be characterised as less demanding in the design process. Namely, easy implementation of the control system is possible using a simple on/off electromagnetic valve. Hence, a high potential could be indicated for application in the current transcritical booster R744 systems, such as in local retail points or the food processing industry.

Numerical analysis of the ejector with closed and open bypass ducts delivered additional data on the prototype device. First, the pressure distribution in the case of the closed bypass duct resulted in unfavourable choking of the mixing section. Reduction of the shock train generation after bypass duct opening provided higher pressure values and unblocked the flow in the mixing cross section. Similar conclusions were reached in a previous numerical study [35].

Simulations of the R744 flow in the suction and bypass chambers revealed a potential for further improvement. Disordered and highly turbulent flow in the latter chamber was correlated with the cross-sectional shape of the channels, which led to flow from the suction chamber. This region could be the basis for an optimisation study of the investigated device.

Further work could include an enhanced analysis of ejectors designed for systems characterised by higher cooling capacities and the development of control libraries based on performance mapping. The automatic mechanism of the bypass duct could be connected with the unit's control system as a demonstrative version of the bypass ejector characterised by a higher technology readiness level. Another solution should be considered for the ejector designed for the low-pressure lift to improve the performance under the high-pressure lift conditions.

9. Acknowledgements

The authors gratefully acknowledge the financial support of the National Centre of Science through project No. 2017/27/B/ST8/00945. Scientific work of JB was financed from the budget for science in years 2017–2021, as a research project 08/060/DG17/0140 under the programme *Diamond Grant*. The work of MP was supported by Silesian University of Technology through project No. 08/060/RGJ20/0251.

References

[1] Lorentzen G. The use of natural refrigerants: a complete solution to the CFC/HCFC predicament. International Journal of Refrigeration 1995;18(3):190–7.

[2] United Nations Environment Programme (UNEP) . Montreal Protocol, 1987 1987;.

[3] United Nations Framework Convention on Climate Change (UNFCCC) . Kyoto Protocol, 1997 1997;.

[4] European Commission . Regulation (EU) No 517/2014 of the European Parliament and of the Council of 16 April 2014 on fluorinated greenhouse gases and repealing Regulation (EC) No 842/2006 Text with EEA relevance. Official Journal of the European Union 2014;57:195–230. doi:doi:10.3000/19770677.L_2013.124.eng.

[5] European Commission . EU ratifies Kigali Amendment to the Montreal Protocol | Climate Action. 2018.

[6] Gullo P. Innovative fully integrated transcritical r744 refrigeration systems for a hfc-free future of supermarkets in warm and hot climates. International Journal of Refrigeration 2019;108:283–310.

[7] Minetto S, Cecchinato L, Brignoli R, Marinetti S, Rossetti A. Water-side reversible co2 heat pump for residential application. International Journal of Refrigeration 2016;63:237–50.

[8] Smitt S, Tolstorebrov I, Hafner A. Integrated co2 system with hvac and hot water for hotels: Field measurements and performance evaluation. International Journal of Refrigeration 2020;116:59 – 69.

[9] Villarino JI, Villarino A, Ángel Fernández F. Experimental and modelling analysis of an office building hvac system based in a ground-coupled heat pump and radiant floor. Applied Energy 2017;190:1020–8.

[10] Sooben D, Purohit N, Mohee R, Meunier F, Dasgupta MS. R744 refrigeration as an alternative for the supermarket sector in small tropical island developing states: The case of mauritius. International Journal of Refrigeration 2019;103:264 –73. doi:https://doi.org/10.1016/j.ijrefrig.2019.03.034.

[11] Besagni G, Mereu R, Inzoli F. Ejector refrigeration: A comprehensive review. Renewable and Sustainable Energy Reviews 2016;53:373–407.

[12] Bellos E, Tzivanidis C. A comparative study of CO2 refrigeration systems. Energy Conversion and Management: X 2018;:100002.

[13] Gullo P, Tsamos KM, Hafner A, Banasiak K, Ge YT, Tassou SA. Crossing CO2 equator with the aid of multi-ejector concept: A comprehensive energy and environmental comparative study. Energy 2018;164:236–63.

[14] Gullo P, Hafner A, Banasiak K. Transcritical r744 refrigeration systems for supermarket applications: Current status and future perspectives. International Journal of Refrigeration 2018;93:269–310.

[15] Cao H, ter Brake H. Progress and challenges in utilization of ejectors for cryogenic cooling. Applied Thermal Engineering 2020;167:114783. doi:https://doi.org/10.1016/j.applthermaleng.2019.114783.

[16] Liu Z, Liu Z, Xin X, Yang X. Proposal and assessment of a novel carbon dioxide energy storage system with electrical thermal storage and ejector condensing cycle: Energy and exergy analysis. Applied Energy 2020;269:115067.

[17] Elbel S, Lawrence N. Review of recent developments in advanced ejector technology. International Journal of Refrigeration 2016;62:1–18.

[18] Elbel S, Hrnjak P. Experimental validation of a prototype ejector designed to reduce throttling losses encountered in transcritical R744 system operation. International Journal of Refrigeration 2008;31(3):411–22.

[19] Smolka J, Palacz M, Bodys J, Banasiak K, Fic A, Bulinski Z, et al. Performance comparison of fixed- and controllable-geometry ejectors in a co2 refrigeration system. International Journal of Refrigeration 2016;65:172–82.

[20] Hafner A, Försterling S, Banasiak K. Multi-ejector concept for R-744 supermarket refrigeration. International Journal of Refrigeration 2014;43:1–13. doi:10.1016/j.ijrefrig.2013.10.015.

[21] Banasiak K, Hafner A, Kriezi EE, Madsen KB, Birkelund M, Fredslund K, et al. Development and performance mapping of a multi-ejector expansion work recovery pack for R744 vapour compression units. International Journal of Refrigeration 2015;57:265–76.

[22] Lawrence N, Elbel S. Experimental investigation on control methods and strategies for off-design operation of the transcritical r744 two-phase ejector cycle. International Journal of Refrigeration 2019;106:570–82.

[23] Zhu J, Elbel S. Experimental investigation of a novel expansion device control mechanism: Vortex control of initially subcooled flashing r134a flow expanded through convergent-divergent nozzles. International Journal of Refrigeration 2018;85:167–83.

[24] Zhu J, Elbel S. Experimental investigation into the influence of vortex control on transcritical r744 ejector and cycle performance. Applied Thermal Engineering 2020;164:114418. doi:https://doi.org/10.1016/j.applthermaleng.2019.114418.

[25] Palacz M, Smolka J, Nowak AJ, Banasiak K, Hafner A. Shape optimisation of a two-phase ejector for CO2 refrigeration systems. International Journal of Refrigeration 2017;74:210–21. doi:10.1016/j.ijrefrig.2016.10.013.

[26] Grazzini G, Milazzo A, Mazzelli F. Ejectors for Efficient Refrigeration. Springer; 2018.

[27] Besagni G. Ejectors on the cutting edge: The past, the present and the perspective. Energy 2019;170:998–1003.

[28] Chen W, Chen H, Shi C, Xue K, Chong D, Yan J. A novel ejector with a bypass to enhance the performance. Applied Thermal Engineering 2016;93:939–46. doi:https://doi.org/10.1016/j.applthermaleng.2015.10.067.

[29] Chen W, Chen H, Shi C, Xue K, Chong D, Yan J. Impact of operational and geometrical factors on ejector performance with a bypass. Applied Thermal Engineering 2016;99:476–84. doi:https://doi.org/10.1016/j.applthermaleng.2016.01.074.

[30] Chen W, Huang C, Chong D, Yan J. Numerical assessment of ejector performance enhancement by means of combined adjustable-geometry and bypass methods. Applied Thermal Engineering 2019;149:950–9. doi:https://doi.org/10.1016/j.applthermaleng.2018.12.052.

[31] Chen W, Fan J, Huang C, Liu S, Chong D, Yan J. Numerical assessment of ejector performance enhancement by means of two-bypass inlets. Applied Thermal Engineering 2020;171:115086. doi:https://doi.org/10.1016/j.applthermaleng.2020.115086.

[32] Tang Y, Li Y, Liu Z, Wu H, Fu W. A novel steam ejector with auxiliary entrainment for energy conservation and performance optimization. Energy Conversion and Management 2017;148:210–21. doi:https://doi.org/10.1016/j.enconman.2017.05.076.

[33] Tang Y, Liu Z, Li Y, Shi C, Wu H. Performance improvement of steam ejectors under designed parameters with auxiliary entrainment and structure optimization for high energy efficiency. Energy Conversion and Management 2017;153:12–21. doi:https://doi.org/10.1016/j.enconman.2017.09.067.

[34] Tang Y, Liu Z, Shi C, Li Y. A novel steam ejector with pressure regulation to dredge the blocked entrained flow for performance improvement in med-tvc desalination system. Energy Conversion and Management 2018;172:237–47. doi:https://doi.org/10.1016/j.enconman.2018.07.022.

[35] Bodys J, Smolka J, Banasiak K, Palacz M, Haida M, Nowak AJ. Performance improvement of the r744 two-phase ejector with an implemented suction nozzle bypass. International Journal of Refrigeration 2018;90:216–28. doi:https://doi.org/10.1016/j.ijrefrig.2018.03.020.

[36] Tashtoush BM, Al-Nimr MA, Khasawneh MA. A comprehensive review of ejector design, performance, and applications. Applied Energy 2019;240:138–72.

[37] Smolka J, Bulinski Z, Fic A, Nowak AJ, Banasiak K, Hafner A. A computational model of a transcritical R744 ejector based on a homogeneous real fluid approach. Applied Mathematical Modelling 2013;37(3):1208–24.

[38] Haida M, Palacz M, Bodys J, Smolka J, Gullo P, Nowak AJ. An experimental investigation of performance and instabilities of the r744 vapour compression rack equipped with a two-phase ejector based on short-term, long-term and unsteady operations. Applied Thermal Engineering 2020;185:116353. doi:https://doi.org/10.1016/j.applthermaleng.2020.116353.

[39] Taylor B, Kuyatt C. Guidelines for Evaluating and Expressing the Uncertainty of NIST Measurement Results: Appendix D1. Terminology. Gaithersburg: National Institute of Standards and Technology, Standard Reference Data Program; 2001.

[40] Banasiak K, Hafner A. 1D Computational model of a two-phase R744 ejector for expansion work recovery. International Journal of Thermal Sciences 2011;50(11):2235–47.

[41] Gullo P, Hafner A, Cortella G. Multi-ejector r744 booster refrigerating plant and air conditioning system integration – a theoretical evaluation of energy benefits for supermarket applications. International Journal of Refrigeration 2017;75:164–76. doi:https://doi.org/10.1016/j.ijrefrig.2016.12.009.

[42] Palacz M, Smolka J, Fic A, Bulinski Z, Nowak AJ, Banasiak K, et al. Application range of the HEM approach for CO2 expansion inside two-phase ejectors for supermarket refrigeration systems. International Journal of Refrigeration 2015;59:251–8. doi:10.1016/j.ijrefrig.2015.07.006.